Pergamon

Int. J. Heat Mass Transfer. Vol. 41, No. 17, pp. 2687–2695, 1998

Printed in Great Britain
0017–9310/98 $19.00+0.00

PII: S0017–9310(97)00342–6

Effects of buoyancy and orientation on the flow in a duct preceded with a double-step expansion

YENG-YUNG TSUI† and SHEU-JANG SHU

Department of Mechanical Engineering, National Chiao Tung University, Hsinchu 300, Taiwan, R.O.C.

(*Received* 27 *December* 1996)

Abstract—A numerical method, employing nonstaggered grid arrangement, is incorporated to deal with mixed convection flow in a duct with a double-step expansion at inlet. The walls downstream of the expansion are maintained at a uniform temperature. In the first series of tests, the duct is placed vertically ($\gamma = 0°$), and the buoyancy effect is examined via gradually increasing Grashof number until no converged solution is obtained. With the aid of buoyancy force the recirculating flows behind the sudden expansion attach to the two step walls when the Grashof number is large enough. In the meanwhile, reversed flow is detected in the centerline region. At $Re = 56$ the flow remains symmetric throughout the Grashof numbers tested whereas for $Re = 114$ the flow field may be symmetric or asymmetric, depending on the Grashof number. Also examined is the effect of inclination angle γ for $Ga = 1000$ and 3000. In the horizontal position ($\gamma = 90°$), two recirculations exist behind the two step walls. When $\gamma > 90°$, a number of recirculations are formed on the two side walls and the main stream exhibits a wavy structure. The wavy flow helps enhance heat transfer. The above results for different duct orientations are equally applicable to both heating and cooling flows.

INTRODUCTION

Mixed convection in ducted flow can be found in many applications, such as heat exchangers, electronic cooling systems and solar collectors. In a duct both the velocity and temperature approach a fully developed state at a large distance away from the inlet. The flow structure in the developing stage is affected by the geometry of the inlet. In the past, many studies were concerned with the heat transfer in straight, vertical 2-D channels or circular tubes [1–4] with less effort on the duct flow preceded by a single backward-facing step [5–7]. Studies concerning the flow with a double step at inlet are few in the literature. This has motivated the present study which explores numerically the effects of buoyancy on the flow and heat transfer in a duct preceded with a symmetric sudden expansion.

Under buoyancy-assisted conditions the flow near a heated wall is accelerated, leading to a velocity reduction in the center of the duct due to conservation of flow rate [2, 3]. When the heating is strong enough, a reversed flow may occur at the center region [4]. In contrast, the flow near the duct wall is retarded in opposing flow. In severe cases, the flow can be reversed at the wall [8, 9]. In general, the opposing buoyancy is more likely to induce flow reversal. Several previous studies have been performed to investigate the flow in inclined pipes [10], cylindrical annuli [11] and two-dimensional ducts [12].

When a duct is preceded with a backward-facing step, the flow separates from the step and a recirculation zone is formed downstream. In an aiding flow the velocity near the heated wall in the recirculation region is opposite to the buoyancy direction. Thus, the size of the recirculation zone decreases as the buoyancy force is increased [6, 7]. For the buoyancy force larger than a certain value the recirculation detaches from the heated wall and attaches only to the adiabatic step. It was observed [13, 14] that the reattachment length of the recirculating flow increases as the duct is rotated away from the vertical position. After 180° rotation, the buoyancy force help enhance the reversed flow and the reattachment length reaches its maximum value.

The flow through a symmetric sudden expansion, i.e., a double backward-facing step, is of interest. The experimental studies of Durst *et al.* [15] and Cherdron *et al.* [16] showed that, without introducing buoyancy force, asymmetric flow pattern prevails, with a large recirculating flow behind one step and a small one behind the other, as the Reynolds number becomes sufficiently large. The asymmetric flow field was also captured by Tsui and Wang [17] with the use of numerical method. In their study a symmetric, straight-walled diffuser with various diffusion angles was under consideration. The half diffusion angle of the diffuser ranged from 15–90°. Two Reynolds numbers (56 and 114) and two expansion ratios (3 and 4)

† Author to whom correspondence should be addressed. Tel.: 3 57 12121 ext. 55122. Fax: 3 57 20634.

NOMENCLATURE

g	gravitational acceleration	x, y	Cartesian coordinates
Gr	Grashof number, $\beta g(T_w - T_0)w_1^3/\nu^2$	X, Y	dimensionless Cartesian coordinates, x/w_1, y/w_1
p	pressure	X_n	dimensionless location of peak Nusselt number
P	dimensionless pressure	X_0	dimensionless recirculation length
Pr	Prandtl number, ν/α	X_r	dimensionless reattachment length.
Q	wall heat flux $(\partial\theta/\partial Y)_w$		
Q_{ave}	mean heat flux through the two side walls	Greek symbols	
Re	Reynolds number, $u_s w_1/\nu$	β	thermal expansion coefficient
T	temperature	γ	inclination angle as measured from the vertical axis
T_w	temperature of walls	ΔV	volume of the considered cell
T_0	temperature of inlet air	θ	dimensionless temperature $(T-T_0)/(T_w-T_0)$
u_s	center line velocity at inlet	ν	kinematic viscosity
U, V	dimensionless velocity components in X and Y directions, u/u_s, v/v_s	ρ	fluid density.
w_1	upstream channel height		
w_2	downstream channel height		

were examined. It was reported that as the Reynolds number or the expansion ratio increases, the diffusion angle at which the flow starts to become asymmetric is reduced.

In this study the buoyancy effects on the ducted flow through a symmetric sudden expansion are investigated. The expansion ratio is fixed at three and the Reynolds number is restricted to 56 and 114. The two sided walls downstream of the sudden expansion are heated and subject to uniform temperature. Firstly, the duct system is placed vertically such that the flow is assisted by the buoyancy force. The Grashof number is gradually increased until no converged solution can be obtained. Then, the duct is rotated to examine the effects of orientation. It is noted that the parametric tests conducted by Lin *et al.* [13] and Hong *et al.* [14] were limited in the range $Gr/Re^2 < 0.3$, whereas the parameter Gr/Re^2 can be as high as 4.6 in this study.

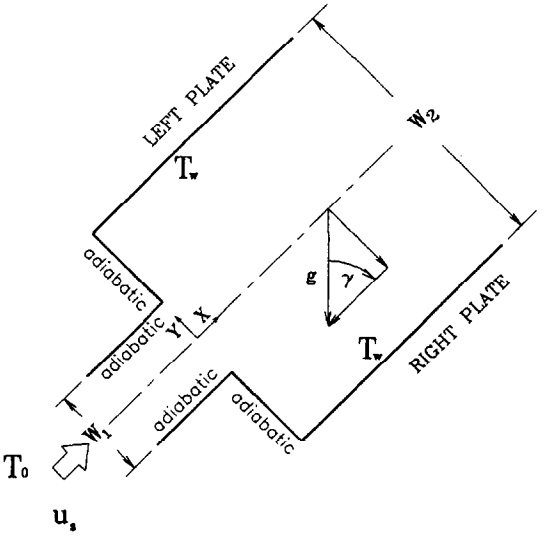

Fig. 1. A schematic drawing of the flow system.

MATHEMATICAL METHOD

The physical model under consideration is illustrated in Fig. 1. Air in a channel with width w_1 is discharged into a larger channel with width w_2 via a double-step sudden expansion. The channel walls are inclined to the gravity direction at an angle γ. It is assumed that the air enters the channel with a uniform temperature T_0 and with a fully developed velocity profile. The centerline velocity at the inlet is denoted as u_s. The walls downstream of the step are maintained at a constant temperature T_w while the other walls are treated adiabatically.

The flow is assumed to be steady, 2-D and laminar, and the Boussinesq approximation is invoked. The governing equations can then be written in the following nondimensional form.

$$\frac{\partial U}{\partial X} + \frac{\partial V}{\partial Y} = 0 \tag{1}$$

$$U\frac{\partial U}{\partial X} + V\frac{\partial U}{\partial Y} = -\frac{\partial P}{\partial X} + \frac{1}{Re}\left(\frac{\partial^2 U}{\partial X^2} + \frac{\partial^2 U}{\partial Y^2}\right) + \frac{Gr\cos\gamma}{Re^2}\theta \tag{2}$$

$$U\frac{\partial V}{\partial X}+V\frac{\partial V}{\partial Y}=-\frac{\partial P}{\partial Y}+\frac{1}{Re}\left(\frac{\partial^2 V}{\partial X^2}+\frac{\partial^2 V}{\partial Y^2}\right)+\frac{Gr\sin\gamma}{Re^2}\theta \quad (3)$$

$$U\frac{\partial \theta}{\partial X}+V\frac{\partial \theta}{\partial Y}=\frac{1}{Re\,Pr}\left(\frac{\partial^2 \theta}{\partial X^2}+\frac{\partial^2 \theta}{\partial Y^2}\right) \quad (4)$$

where

$$X=x/w_1,\quad Y=y/w_1,\quad U=u/u_S,\quad V=v/u_S \quad (5a)$$

$$P=(p+\rho_0 g(x\cos\gamma+y\sin\gamma))/\rho u_s^2,\quad \theta=(T-T_0)/(T_w-T_0) \quad (5b)$$

$$Pr=\nu/\alpha,\quad Re=u_S w_1/\nu,\quad Gr=g\beta(T_w-T_0)w_1^3/\nu^2. \quad (5c)$$

The difference analogues of the governing equations were obtained using the finite-volume method. In the discretization the flow convection was approximated by the linear upwind difference [18] in which the transported value across a cell face is calculated by a linear extrapolation from two nodal points upstream of the considered face. It was shown by Tsui [18] that this second-order accurate scheme can effectively reduce numerical diffusion. The code used in this study was constructed based on nonorthogonal, nonstaggered grids such that it could cope with irregular flow geometry. It is well known that with the nonstaggered grid arrangement the velocity and pressure are coupled only in a checkboard manner and, thus, it may produce oscillation in velocity and pressure. To avoid this problem the momentum interpolation method of Rhie and Chow [19] was incorporated to calculate the velocities through cell faces. The face velocities were then forced to satisfy the continuity to yield a pressure-correction equation. By this method, all the terms of face velocity equations except the pressure gradients are yielded via linear interpolation using the momentum equations for the two grid points adjacent to the face. The pressure gradients are approximated by central difference using the nearby nodal pressures. It is noted that if nonuniform grid is used, the linear interpolation procedure is not suitable for calculation of buoyancy force terms. As shown in Fig. 2, the control volume represented by the face point "e" occupies half P-cell and half E-cell. Thus, the volume of this cell is equal to the mean of the two adjacent cell volumes. Instead of using linear interpolation, an averaging approach must be employed [20] for approximating buoyancy terms to conserve the body force field. This is written as, e.g., for the U-momentum equation,

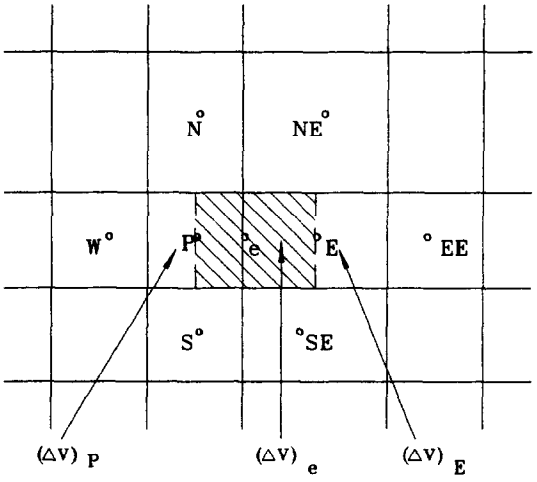

Fig. 2. Illustration of control volume for a face point.

$$\left(\frac{Gr\cos\gamma}{Re^2}\theta\Delta V\right)_e=\frac{1}{2}\left[\left(\frac{Gr\cos\gamma}{Re^2}\theta\Delta V\right)_P+\left(\frac{Gr\cos\gamma}{Re^2}\theta\Delta V\right)_E\right]. \quad (6)$$

RESULTS AND DISCUSSION

To validate the solution method described above the flows over a single backward-facing step investigated by Lin *et al.* [6] and Hong *et al.* [14] have been reproduced. In the former study the duct system was vertically placed. Figure 3 provides a comparison of the flow reattachment length X_r of the recirculation flow behind the step, the length X_0 of the secondary recirculation at the step corner, and the location of maximum heat transfer X_n for various values of Gr/Re^2. It is seen that good agreement between the two predictions is obtained. The flow system was rotated in the study of Hong *et al.* [14]. The predicted reattachment length against the orientation is compared

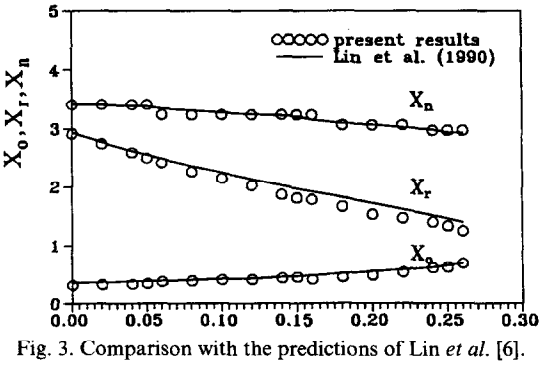

Fig. 3. Comparison with the predictions of Lin *et al.* [6].

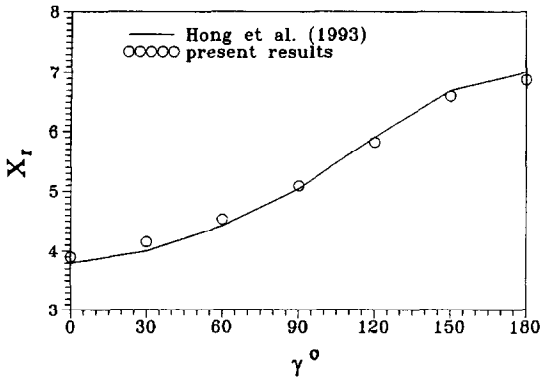

Fig. 4. Comparison with the predictions of Hong *et al.* [14].

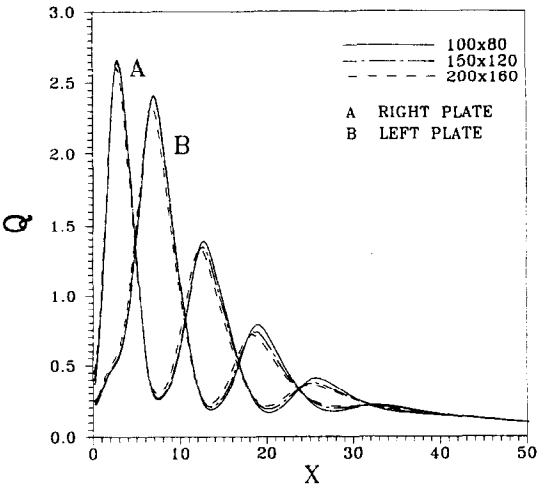

Fig. 5. Grid refinement tests for $\gamma = 180°$, $Gr = 1000$, and $Re = 114$.

in Fig. 4. The agreement between the two studies appears to be quite good. The above results justify the numerical method used in this study.

In the present investigation of the flow through a double backward-facing step, the expansion ratio (W_2/W_1) is fixed at three. The Prandtl number is assumed to be 0.7 and two Reynolds numbers are considered: 56 and 114. The overall length of the computational domain is $55W_1$ and the part downstream of the expansion is $50W_1$. This length has been found to be long enough for the outlet to be away from the recirculating flows generated in the duct. Results shown in the following verify that the flow becomes nearly fully developed at the exit of the duct. Therefore, zero streamwise gradients are imposed there as outlet boundary conditions.

The results presented below are divided into two parts. The first is to examine the effects of buoyancy force on aiding flows for which the inclination angle $\gamma = 0°$, i.e., the flow is directed upward. The Grashof number is gradually increased until no converged solution can be found. The maximum Gr allowed for $Re = 114$ is 60 000 and that for $Re = 56$ is 10 000. In the second, the effects of orientation are examined by varying the inclination angle γ from 0–180° for $Gr = 1000$ or 3000. In the following, selected results are presented. More information can be found in Shu [21].

Grid refinement tests have been performed for the case with $Re = 114$, $Gr = 1000$ and $\gamma = 180°$. In Fig. 5 the distributions of heat transfer rate ($Q = |\partial\theta/\partial Y|_{wall}$) across the two side walls are shown. There is no significant difference among the results for the three meshes used. In the following the predictions using 150×120 grid are presented.

Effects of Grashof number

The streamlines for $Gr = 100, 400, 2000, 10\,000$ and 50 000 with $Re = 114$ and $\gamma = 0°$ are illustrated in Fig. 6. At the lowest Grashof number $Gr = 100$, an asymmetric flow field is detected, with two different sizes of recirculating flow behind the steps. This kind of flow pattern is similar to that seen in Durst *et al.* [15] and Tsui and Wang [17], in which forced convection ($Gr = 0$) was considered. The cause of the asymmetry is due to the instability of the shear layers separating the main stream and the two recirculation flows behind the two steps. There exists a point of inflection in the velocity profile, which is a necessary condition for instability according to the Rayleigh's inviscid theory [22]. Small disturbances embedded in a shear layer may be amplified to form vortex-like structure, as observed by Sato [23] and Browand [24] in a boundary layer flow separating from a step. Due to confinement of the duct the two shear flows in the present case affect each other. The interaction of the two layers results in alternating shedding of vortices and, thus, flow asymmetry [16]. In numerical calculations a source to cause asymmetric perturbation is the roundoff error and another is due to the relaxation

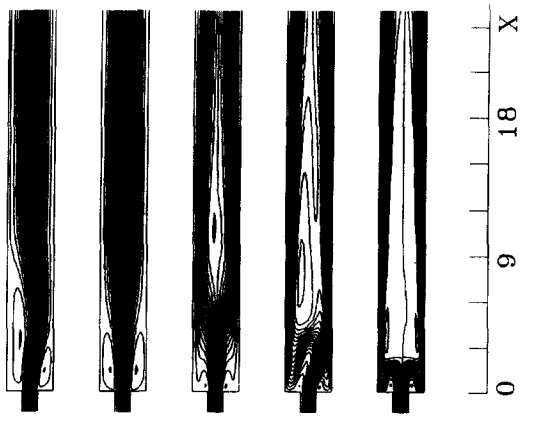

Fig. 6. Flow streamlines for various Grashof numbers with $\gamma = 0°$ and $Re = 114$.

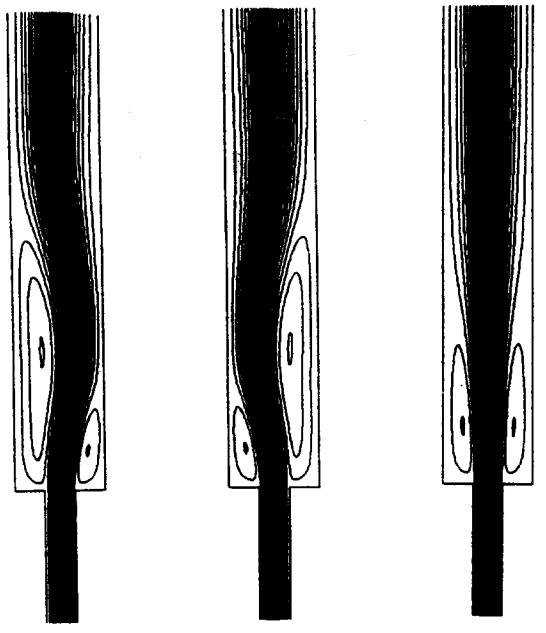

Fig. 7. Three possible solutions for $Gr = 0$, $\gamma = 0°$ and $Re = 114$.

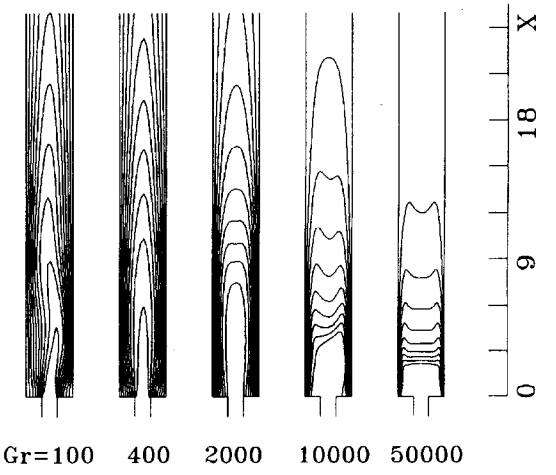

Fig. 8. Isotherms for various Grashof numbers with $\gamma = 0°$ and $Re = 114$.

scheme. In Fig. 7 three calculated results are presented for the case of forced convection. These solutions are obtained using SLR (successive line relaxation) which adopts the TDMA (tridiagonal matrix algorithm) as the relaxation scheme. On each grid line the TDMA behaves as a direct solver. In the first a vertical SLR (directed from inlet to exit) is incorporated to sweep from the left plate to the right plate, resulting in a larger recirculating eddy behind the left step. In the second the computational domain is swept by the vertical SLR from the right to the left. A seen in the figure, the two solutions are identical except that the flow patterns are reversed. When a horizontal SLR is used, the symmetric solution is obtained because this relaxation scheme behaves as a symmetric solver. The above results demonstrate that with an asymmetric solver the solution would not be symmetric and the solution pattern may depend on the sweeping direction. It should be noted that under severe conditions, such as in the buoyancy-opposed flow with large Grashof numbers, asymmetric solutions are always detected. This implies that flow instability can be triggered by such a small disturbance of roundoff error.

As seen in Fig. 6, the buoyancy force helps limit the growth of the instability where the Grashof number is low. At $Gr = 400$ the two recirculation regions are of the same size, being larger than the small recirculation and smaller than the larger one of the $Gr = 100$ flow. As Gr is further increased, the reattachment length decreases and approaches zero. For $Gr > 2000$ the recirculations are restricted to the backward-facing steps, which has been observed by Lin *et al.* [6] and Baek *et al.* [7]. Since the flows near the walls are largely accelerated by the increased buoyancy force, a reversed flow is formed in the centerline region downstream of the double step because mass flux must be conserved at each axial location. As a consequence, inflection points appears in the velocity profile at the edges of the recirculating flow. This triggers instability again and causes the flow to deviate from symmetry. However, as the Grashof number becomes very high ($Gr = 50\,000$), symmetric pattern returns. The central region becomes nearly stagnant, as will be apparent in viewing velocity profiles given latter, and a pair of recirculation zones are located between the stagnation central region and the wall flows.

In Fig. 8 isotherms are presented. Apparently, the contour patterns are closely related to the flow structure represented by the streamlines. The axial velocity profiles at $X = 5W_1$ are given in Fig. 9. As expected, the profiles for $Gr = 100$ and $10\,000$ are not symmetric while those for $Gr = 2000$ and $40\,000$ exhibit good

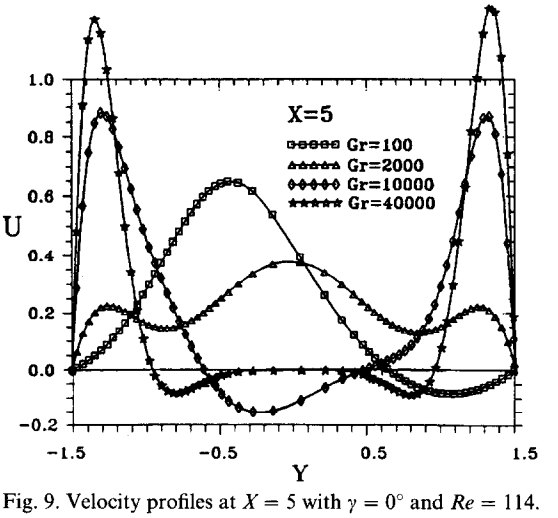

Fig. 9. Velocity profiles at $X = 5$ with $\gamma = 0°$ and $Re = 114$.

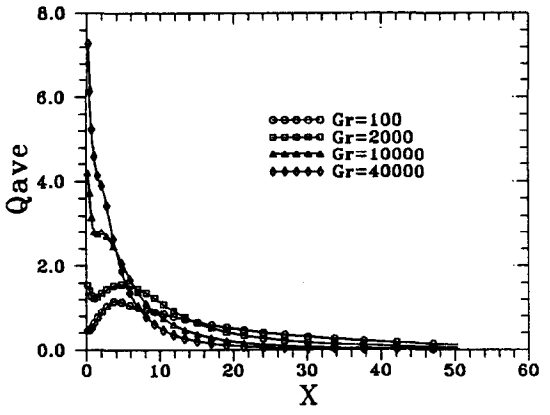

Fig. 10. Heat transferred through the walls with $\gamma = 0°$ and $Re = 114$.

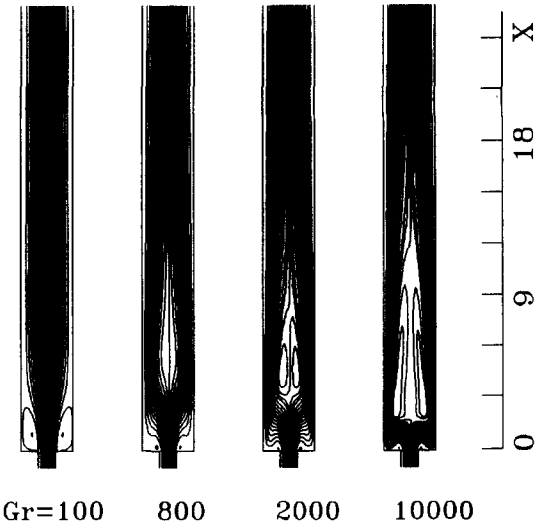

Fig. 11. Flow streamlines for various Grashof numbers with $\gamma = 0°$ and $Re = 56$.

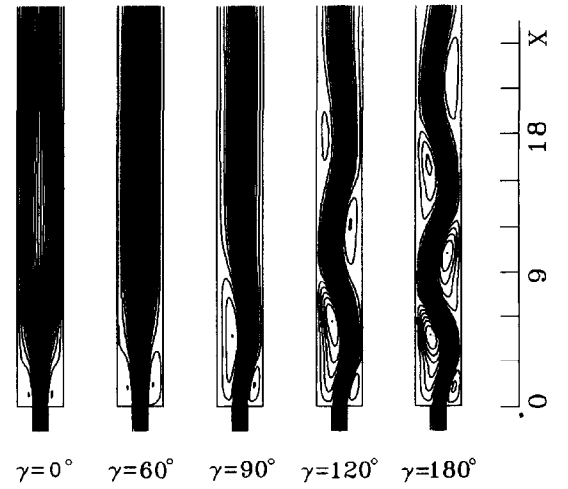

Fig. 12. Flow streamlines for various inclination angles with $Gr = 1000$ and $Re = 114$.

symmetric behavior. It is interesting to notice that for $Gr = 40\,000$ the flow in the center region between the two reversed flows is nearly stagnant.

The axial variation of the heat flux ($Q = |\partial\theta/\partial Y|_{wall}$) averaged over the two side walls is presented in Fig. 10. The heat flux increases with Gr in the initial stage near the inlet and decreases more quickly for the high Gr cases. It is noted that the areas under the curves represent total heat transfers into the duct. The total heat added in must be the same, irrespective of Grashof number, if the fully developed state (i.e. $\theta = 1$) is reached at the outlet. From this point of view it is not surprising that the heat transfer rate is low in the late stage if it is high near the inlet. The location of the peak Q for the low Grashof number ($Gr = 100$) roughly correspond to the reattachment point of the smaller recirculation zone because the flow emerging from the inlet behaves like a jet and impinges on the wall around that location. According to the streamline plots shown in Fig. 6, when the Grashof number increases, the reattachment point moves upstream and finally the recirculation is limited to the step for Gr larger than 2000. This results in that a part of the jet flow turns its direction to sweep across the step corners. Due to the combined effects of the jet-like flow and the turning flow in the $Gr = 2000$ and 10 000 cases the heat transfer rate, being high at the corners, declines first, followed by a rise, and finally decreases to the fully developed stage. For $Gr = 40\,000$ the entire flow turns immediately at the entrance, resulting in monotonic attenuation of the heat transfer.

As the Reynolds number reduces to 56, the relatively large viscosity restricts the growth of instability and, thus, the flow exhibits symmetric patterns, as evidenced in the studies of Durst *et al.* [15] and Tsui and Wang [17]. The heat added does not change the situation, as can be seen in Fig. 11. At low Grashof number ($Gr = 100$), the two recalculation zones are of the same size. Similar to the case with $Re = 114$, when the Grashof number becomes sufficiently large, the two recirculations are limited to the steps and flow reversal takes place in the center region. However, different from the high Re flows, a pair of equal-strength recirculations are always detected at the centerline, as seen at $Gr = 2000$ and 10 000.

Effects of orientation

Streamlines for $Re = 114$ and $Gr = 1000$ at various inclination angles are sketched in Fig. 12. As indicated previously, the buoyancy force assists to stabilize the flow at this Grashof number and render the flow symmetric at $\gamma = 0°$. When the duct system is inclined to the vertical position, the buoyancy forces exerted on both sides of the duct are not of the same magnitude. However, the symmetry is maintained for small γs despite the asymmetric buoyancy force distribution because this force is relatively small, comparing with

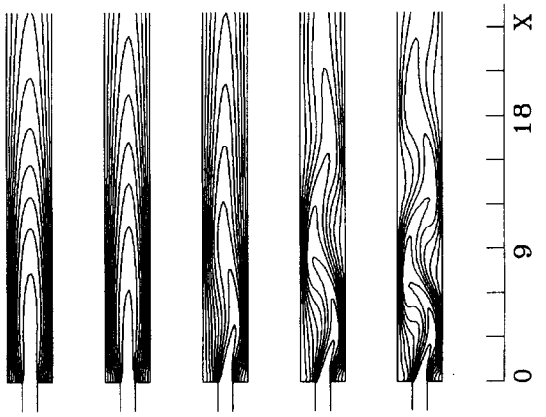

$\gamma=0°$ $\gamma=60°$ $\gamma=90°$ $\gamma=120°$ $\gamma=180°$

Fig. 13. Isotherms for various inclination angles with $Gr = 1000$ and $Re = 114$.

the inertia force ($Gr/Re^2 = 0.077$). It is seen that the flow pattern only slightly deviates from symmetry at $\gamma = 60°$. By positioning the duct horizontally ($\gamma = 90°$), the flow structure becomes fully asymmetric, with a small recirculation on the bottom wall (the right plate in Fig. 1) and a large one on the top. When the inclination angle is further increased, the component of the buoyancy force in the x direction opposes the flow direction. In this opposing flow, the flow is prone to instability. As a result, new recirculation zones appear. As seen in the figure, on each side wall there exits two recirculations at $\gamma = 120°$. By 180° the buoyancy force is directly opposite to the flow direction and the number of recirculations is increased to three. The isotherms are portrayed in Fig. 13. Obviously, the contours are shaped by the flow streamlines.

The heat transfers through the two walls for $\gamma = 0$ and 90° are given in Fig. 14. At $\gamma = 0°$ the symmetric flow leads to collapse of the two curves into one while different curves are visible for $\gamma = 90°$. The much larger peak value seen on the right plate in the latter is caused by the impingement of the jet-like flow on

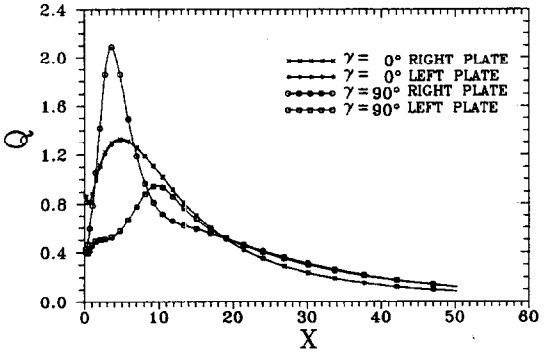

Fig. 14. Heat transferred through the walls for $\gamma = 0°$ and 90° with $Gr = 1000$ and $Re = 114$.

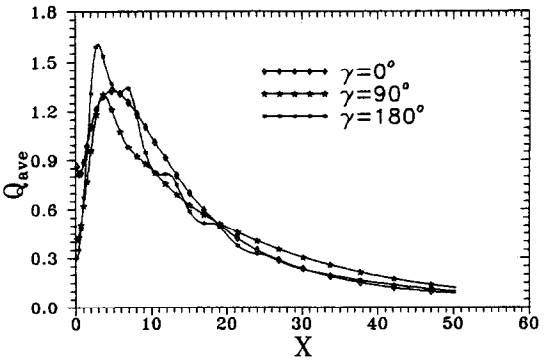

Fig. 15. Comparison of mean heat transferred along the walls for $Gr = 1000$ and $Re = 114$.

the wall. The results for $\gamma = 180°$ can be seen in Fig. 5. The oscillation reflects the wavy flow seen in Fig. 12. The peaks correspond to the positions where the main stream sweeps across the walls and the troughs are related to the recirculation centers. The peak values quickly decay with the axis. Comparison of the heat transfers averaged over the two plates for the three cases is made in Fig. 15. As mentioned above, the areas under the curves stand for the total heats added in and the total heat transfers must be equal provided that the temperature profiles at the exit of the duct are the same. Based on this understanding, the low level of heat transfer near the outlet for $\gamma = 0°$ simply reflects that it is superior to the other orientations. It is interesting to observe that the wavy flow helps to enhance heat transfer for $\gamma = 180°$, making it more effective than the $\gamma = 90°$ case and comparable with that of $\gamma = 0°$.

It was just observed that when the Grashof number is greater than 2000 in the aiding flow, flow reversal is formed in the centerline region and asymmetric structure appears. This can be seen from Fig. 16 in which the streamlines for $Gr = 3000$ are shown. By

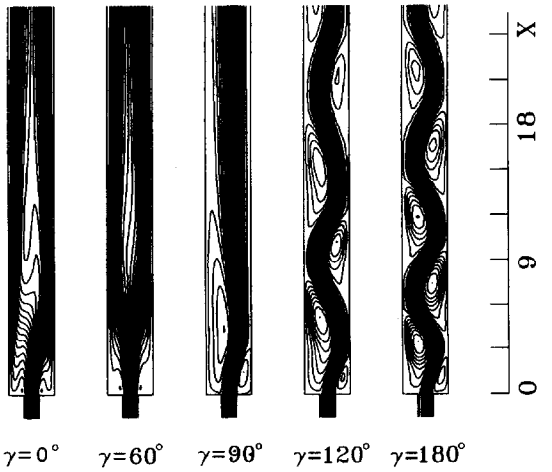

$\gamma=0°$ $\gamma=60°$ $\gamma=90°$ $\gamma=120°$ $\gamma=180°$

Fig. 16. Flow streamlines for various inclination angles with $Gr = 3000$ and $Re = 114$.

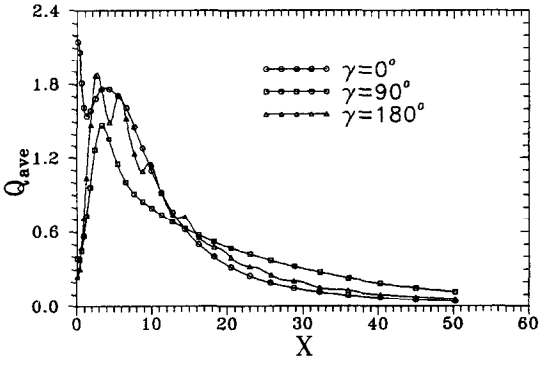

Fig. 17. Comparison of mean heat transfers along the walls for $Gr = 3000$ and $Re = 114$.

rotating the duct, the reversal gradually diminishes and completely disappears at $\gamma = 60°$. It is interesting to notice from Figs. 12 and 16 that the inclination angle 60° seems to be a critical value. At this angle symmetric flow patterns prevail. However, this critical angle may depend on Reynolds number. In the horizontal direction, just like the low Re case, a large and a small recirculating flows appear behind the steps. Further increase in inclination angle results in a wavy flow with a number of recirculations residing on the side walls. The number of recirculations increases with the Grashof number and inclination angle. At $\gamma = 180°$, there are four recirculations on the left wall and five on the right (being truncated in Fig. 16). For the opposing flow it is difficult to obtain converged solution for Grashof number greater than 3000 whereas, for the aiding flow, steady-state solution is possible for Gr up to 60 000. It implies that the opposing flow is more sensitive to the flow instability and is prone to become unsteady [8, 9]. The average heat fluxes across the walls shown in Fig. 17 demonstrate that the wavy structure of the opposing flow brings about more effective heat transfer than the horizontal duct does. However, the aiding flow is still the most preferred.

In the above the results are presented for $0° \leqslant \gamma \leqslant 180°$. Since the duct geometry and the imposed boundary conditions are symmetric to the centerline, the flow for an inclination angle γ in the range between 180° and 360° is simply given by the flow for an angle of $360° - \gamma$, in which the roles of the right and left walls are interchanged. It is easy to see that when the angle γ is replaced by $360° - \gamma$, the buoyancy force in the x direction ($Gr \cos \gamma$) is unchanged and that in the y direction ($Gr \sin \gamma$) becomes negative. Owing to the symmetric configuration, it does not matter if the y component is negative or not. It is also interesting to note that the above results are applicable to both heating as well as cooling flows. In view of the following identities,

$$Gr \cos\gamma = -Gr \cos(180° + \gamma) \quad (7a)$$

$$Gr \sin\gamma = -Gr \sin(180° + \gamma) \quad (7b)$$

a heating flow with a positive Gr at an inclination angle γ is equivalent to a cooling flow with a negative Gr at an inclination angle $180° + \gamma$.

CONCLUSIONS

A mathematical method has been developed to investigate the mixed convection flow through a double-step sudden expansion and into a duct with a uniform temperature imposed on the walls. Based on the calculated results, the following conclusion can be drawn.

(1) For buoyancy-assisted flow heat transfer helps accelerate the flow near the heated wall and flow reversal takes place in the centerline region as the Grashof number becomes high enough. When the duct is placed vertically, the flow field remains to be symmetric throughout the Grashof number range tested for $Re = 56$. A pair of recirculating flows appear near the centerline as Gr becomes sufficiently large. At $Re = 114$ the asymmetric flow seen in the forced convection is first transformed to become symmetric at low Grashof numbers. It is followed by appearance of a single reversed flow in the centerline region and asymmetric pattern prevails again. By further increasing Grashof number the flow returns to become symmetric, with a pair of recirculations being adjacent to the high-speed near-wall flows. In the centerline region between the two recirculations the flow is nearly stagnant.

(2) When the duct is inclined to the vertical position, a symmetric pattern is obtained at $\gamma = 60°$. However this critical angle may depend upon Reynolds number. In the horizontal position ($\gamma = 90°$) different sizes of recirculation appear behind each side of the expansion. For $\gamma > 90°$ the opposing buoyancy force give rise to a number of recirculations on the two side walls, and the main stream exhibits a wavy structure. The heat transfer peaks at the locations where the wavy flow attaches to the walls and is low in recirculation regions. The overall heat transfer is enhanced by the wavy flow, compared with the horizontally placed duct.

(3) Due to the symmetric arrangement the present results for heating flow are also applicable to cooling flow.

Acknowledgement—The authors wish to acknowledge the support of the National Center for High-Performance Computing for providing computer resources.

REFERENCES

1. Lawrence, W. T. and Chato, J. C., Heat transfer effects on the developing laminar flow inside vertical tubes. *ASME Journal of Heat Transfer*, 1966, **88**, 214–222.
2. Aung, W. and Worku, G., Developing flow and flow reversal in a vertical channel with asymmetric wall tem-

peratures. *ASME Journal of Heat Transfer*, 1986, **108,** 299–304.
3. Habchi, S. and Acharya, S., Laminar mixed convection in a symmetrically or asymmetrically heated vertical channel. *Numerical Heat Transfer*, 1986, **9,** 605–618.
4. Ingham, O. B., Keen, D. J. and Heggs, P. J., Two-dimensional combined convection in vertical parallel plate ducts, including situations of flow reversal. *International Journal of Numerical Methods in Engineering*, 1988, **26,** 1645–1664.
5. Sparrow, E. M. and Chuck, W., PC solutions for heat transfer and fluid downstream of an abrupt, asymmetric enlargement in a channel. *Numerical Heat Transfer*, 1987, **12,** 19–40.
6. Lin, J. T., Armaly, B. F. and Chen, T. S., Mixed convection in buoyancy-assisting, vertical backward-facing step flows. *International Journal of Heat and Mass Transfer*, 1990, **33,** 2121–2131.
7. Baek, B. J., Armaly, B. F. and Chen, T. S., Measurements in buoyancy-assisting separated flow behind a vertical backward-facing step. *ASME Journal of Heat Transfer*, 1993, **115,** 403–408.
8. Chang, T. S. and Lin, T. F., Steady and oscillatory opposing mixed convection in a symmetrically heated vertical channel with a low-Prandtl number fluid. *International Journal of Heat and Mass Transfer*, 1993, **36,** 3783–3795.
9. Lin, T. F., Chang, T. S. and Chen, Y. F., Development of oscillatory asymmetric recirculating flow in transient laminar opposing mixed convection in a symmetrically heated vertical channel. *ASME Journal of Heat Transfer*, 1993, **342,** 342–352.
10. Lavine, A. S., Kim, M. Y. and Shores, C. N., Flow reversal in opposing mixed convection flow in inclined pipes. *ASME Journal of Heat Transfer*, 1989, **111,** 114–120.
11. Bohne, D. and Obermeier, E., Combined free and forced convection in a vertical and inclined cylindrical annulus. *Proceedings of the 8th International Heat Transfer Conference*, ed. C. L. Tien, V. P. Carey and J. K. Ferrel, 1986, **3,** 1401–1406.
12. Maughan, J. R. and Incropera, F. P., Experiments on mixed convection heat transfer for airflow in a horizontal and inclined channel. *International Journal of Heat and Mass Transfer*, 1987, **30,** 1307–1318.
13. Lin, J. T., Armaly, B. F. and Chen, T. S., Mixed convection heat transfer in inclined backward-facing step flows. *International Journal of Heat and Mass Transfer*, 1991, **34,** 1568–1571.
14. Hong, B., Armaly, B. F. and Chen, T. S., Laminar mixed convection in a duct with a backward-facing step: the effects of inclination angle and Prandtl number. *International Journal of Heat and Mass Transfer*, 1993, **36,** 3059–3067.
15. Durst, F., Melling, A. and Whitelaw, J. H., Low Reynolds number flow over a plane symmetric sudden expansion. *Journal of Fluid Mechanics*, 1974, **64,** 111–128.
16. Cherdron, W., Durst, F. and Whitelaw, J. H., Asymmetric flows and instabilities in symmetric ducts with sudden expansions. *Journal of Fluid Mechanics*, 1978, **84,** 13–31.
17. Tsui, Y. Y. and Wang, C. K., Calculation of laminar separated flow in symmetric two-dimensional diffusers. *ASME Journal of Fluids Engineering*, 1995, **117,** 612–616.
18. Tsui, Y. Y., A study of Upstream-weighted high-order differencing for approximation to flow convection. *International Journal for Numerical Methods in Fluids*, 1991, **13,** 167–199.
19. Rhie, C. M. and Chow, W. L., Numerical study of the turbulent flow past an airfoil with trailing edge separation. *AIAA Journal*, 1983, **21**(11), 1525–1532.
20. Tsui, Y. Y. and Lin, J. Y., Flow calculation using non-staggered grids. *Proceedings of the 8th National Conference of the CSME*, 1991, **1,** 29–36.
21. Shu, S. J., Mixed-convection calculation in a two-dimensional duct preceded by symmetric diffusers. M.Sc. thesis, National Chiao Tung University, 1995.
22. White, F. M., *Viscous Fluid Flow*, Chap. 5. McGraw-Hill, New York, 1991.
23. Sato, H., Experimental investigation on the transition of laminar separated flow. *Journal of the Physical Society of Japan*, 1956, **11.**
24. Browand, F. K., An experimental investigation of the instability of an incompressible, separated shear layer. *Journal of Fluid Mechanics*, 1966, **26,** 281–307.